

A proposal for Compton Electron Detector R&D

Stephan Aune⁹, Alexandre Camsonne¹, Wouter Deconinck⁸,
Dipankar Dutta⁴, Greg B. Franklin⁷, David Gaskell¹, Cynthia
Keppel¹, Krishna Kumar⁶, Fanglei Lin¹, Juliette Mammei², Dustin
McNulty³, Vasilyi Morozov¹, Kent Paschke⁵, Brian Quinn⁷, and
Seamus Riordan⁶

¹ Thomas Jefferson National Accelerator Facility

² University of Manitoba

³ Idaho State University

⁴ Mississippi State University

⁵ University of Virginia

⁶ Stony Brook University

⁷ Carnegie Mellon University

⁸ College of William and Mary

⁹ SEDI CEA Saclay

June 27, 2014

1 Proposal

This proposal spans over a period of three years. The testing method will measurement in parasitic or during actual Compton measurement. The energy range covered will be the one from JLAB 12 GeV which in Hall A goes from 2.2 GeV to 11 GeV. Most of the time we will use the current of the running experiment, some high current running could be arranged for short period. This would be a test of Compton measurement accuracy. Though since current will be limited to around $100 \mu\text{A}$, rates will be of the order of 100 KHz maximum. In order to test the high rate capability and radiation hardness, we will also use low current straight beam through the detector at low current. The injector can deliver 10 pA of beam with a control of the charge asymmetry at the 0.1 % level, by generating a charge asymmetry of a few percent one can evaluate the accuracy of the detector in integrated mode. At 10 pA rates will be of the order of 60 MHz. Another way to test the detector punctually would be to place the detector behind the parity detectors in the spectrometers during parity experiments in those case the rate could be varied more easily.

1.1 Deliverables of the proposal

This proposal is focusing on the polarimetry of the electron beam through Compton by detecting the Compton electrons. The goals are :

- demonstrate we can reach 1% level polarimetry in the 7 to 11 GeV energy range which overlaps with first stage EIC energy range.
- test and develop detector technologies which can withstand the radiation and rates generated at EIC or are cheap and accessible to be replaced.
- test the performance of an integrated method against an event by event measurement.
- determine the effect of a thin window on polarization measurement to study the option to have the same Roman pot detector design to detect forward particles and Compton polarimetry.
- As a conclusion of this project, a test bed for Compton polarimetry will be available at Jefferson Laboratory for the R&D of EIC Compton polarimetry during the whole 12 GeV program at Jefferson Laboratory.

1.2 Work / split assignement

- study of the detector placement with the Vasilyi Morozov and Fanglei Lin
- Diamond detector will be procured and build by Juliette Mammei with help of Dipangkar Dutta
- Micromegas based prototype will be designed and build by CEA Saclay Stephan Aune

- The vacuum chamber will be built by Jefferson Laboratory
- Detector simulation and tests will be carried by Alexandre Camsonne and David Gaskell from Jefferson Laboratory
- Quartz detector will be built by Dustin McNulty with help Krishna Kumar, Seamus Riordan
- Quartz detector FADC based readout will be taken care of by Brian Quinn, Gregg B. Franklin and Wouter Deconinck.
- Roman pot design will be done by Alexandre Camsonne with Hall A Jefferson Laboratory designers and built by Jefferson Laboratory.
- Funding for a graduate student will be asked to carry out the simulation, detector work and test on an instrumental thesis.

1.3 First year 2015

1.3.1 Diamond strip detector

We are requesting funds for two diamond detector planes for testing the high rate capability, the performance of the detector in integrating mode and radiation hardness.

1.3.2 First quartz detector test

As mentioned previously, the PREX experiment used a small quartz detector to measure. We are planning to reuse the same detector as PREX to demonstrate the feasibility and the accuracy of an integrated measurement using such detector. We will begin with test of the detector in vacuum so an APD and a SiPM will be acquired and tested for linearity and first detector tests in vacuum.

1.3.3 Micromegas prototype

The two prototypes will be manufactured at CEA Saclay. They will take care of the GERBER creation. Produce the Micromegas and test it in their laboratory and ship it to Jefferson Laboratory for Compton measurement.

1.4 Second year

1.4.1 Scattering chamber

From the experience of Hall A with silicon strip detector we lean toward a diamond detector. We propose to modify the scattering chamber in Hall A to be similar to the Hall C chamber which is compatible with the use of diamond detectors. Indeed the electrical signal from a diamond detector is much smaller than silicon. So the cable length needs to be kept short in order to reduce the capacitance to have the best signal to noise ratio. The top flange will be modified

so it could accept different detectors to be tested. This would allow the detector testing either in Hall A or Hall C which would allow flexibility since usually only one parity experiment is run at the same time. If fund are available this could be skipped and a roman pot design could be designed from the start but the cost of the first year would be significantly increased.

1.4.2 New quartz detector

After the initial test we plan to request 20 K\$ to fabricate a detector optimized for the Compton measurement.

1.5 Third year

For the third year the we will ask for the funding to build a roman pot so detectors could be easily swapped for testing and allowing to test atmospheric gaseous detectors.

1.6 Funding request

Year	Detector	Amount
2015	Diamond strip	45 K\$
2015	Micromegas prototype	20 K\$
2015	Quartz readout	15 K\$
2015	Graduate student	30 K\$
2015	Travel fund	15 K\$
2015	Total	125 K\$
2016	Vacuum Chamber	45 K\$
2016	Quartz dedicated integrating detector	20 K\$
2015	Graduate student	30 K\$
2016	Travel fund	15 K\$
2016	Total	110 K\$
2017	Roman pot	185 K\$
2015	Graduate student	30 K\$
2017	Travel fund	15 K\$
2017	Total	230 K\$
Total		465 K\$

This includes 54.5% of overhead on the first 50 K\$.

2 Motivation for Compton polarimetry

As mentioned in the proposal “RD 2013-6: R&D Proposal for an electron polarimeter, a luminosity monitor and a low Q²-tagger” . Precision electron polarimetry can have a significant impact on measurements at EIC for example in the measurement of luminosity which could be affected. In the white paper section 4.3 and 6.2.5, the accuracy on the polarization is aimed to be at 1%. The best Compton measurement was done at SLC which reached 0.5 % but at a higher energy of 46.2 GeV. However the condition at Stanford were quite different to an EIC machine : beam and laser were pulsed at a few hertz and the scattered electron displacement was of the order of centimeters in addition to the high energy. At lower energy and with Continuous Wave beam at Jefferson Laboratory 1% level accuracy was achieved at 6 GeV. We anticipate accuracy at this level at 12 GeV, the higher background levels being counterbalanced by a larger analyzing power at higher energies.

3 Requirements for Compton polarimetry at EIC

In order to monitor the polarization of the electron, Compton Scattering is ideal. This process is a perfectly computable QED process which allows a non invasive and continuous monitoring of the polarization. The electron beam interacts with a source of circularly polarized photons : either a laser or using a cavity to amplify a seed laser. The cross section of the Compton process is dependent on the electron helicity, by measuring the asymmetry between two opposite longitudinal helicities and computing the analyzing power of the Compton process one can extract the polarization. In order to detect both photons and electrons a dipole magnet is used after the interaction allowing to catch the Compton photons in the zero degree line and the Compton electrons which are deflected more than the beam after giving energy to the photon during the Compton interaction.

4 eRHIC

The electron beam of eRHIC will be a multipass Energy Recovery Linac with a repetition rate of 10.8 MHz. This design is very close to the Jefferson Laboratory design. Nominal current will be as high as 50 mA by using the “gatling gun” design where several sources are used at the same time by switching to another source for each bunch. The helicity of the beam can be easily switched by using a pockel cell at the laser source. Since each source can have different polarization a logic signal for each source will be used to measure the average polarization of each one. The detectors should be optimized for a fast response less than 100 ns to be able to resolve each source.

5 MEIC

The MEIC is a ring ring collider. The electron beam is filled from the 12 GeV CEBAF. The beam bunch is 748.5 MHz repetition rate. The beam will be divided in two helicity macro train of $2.3 \mu s$. By integrating the Compton signal on each macro train and computing the asymmetry one can determine the average polarization of the two macrobunch trains. It is possible that a finer time structure will be used to have more flip of the spin over time. Also local polarization measurement will be possible since the same bunch are circulating several times in the machine allowing to increase the statistic over several turns.

6 Background Simulation

Since we have an electron beam, the background is mostly coming from Synchrotron radiation which manages to bounce in the detector, Bremsstrahlung in the non perfect vacuum and interaction with the halo of the beam. Simulation work was started using the Hall C Compton simulation. First results for the background are shown in plots Fig.1 one can see the contributions of the different background in the photon detector (top plot) and in the electron detector (bottom plot) at 3 GeV with a virtual cavity without any aperture. The red curve is the background coming from Brehmstrahlung, in blue we have the Compton signal and in purple the beam halo contribution. At 3 GeV signal to noise ratio is about 1000 for photon and above 1000 for the electron detector after strip 40.

In Fig.2, apertures for the cavity were added with a 1 cm diameter. In this case the background generated from the halo is about the same order as the signal, so particular attention must be taken in the design of the beamline to limit the background due to the halo.

In Fig.3, we have a higher energy beam of 5 GeV with an aperture of 2 cm.

The electron detector has a better signal to background ratio than the photon detector. With the 2 cm aperture the halo and with a focusing of the beam at the interaction point we see little to none contribution from halo.

7 Compton rates

The Compton rates were evaluated using Compton cross section assuming the beam collides with a green (532 nm) laser with a crossing angle of 1.3 degrees.

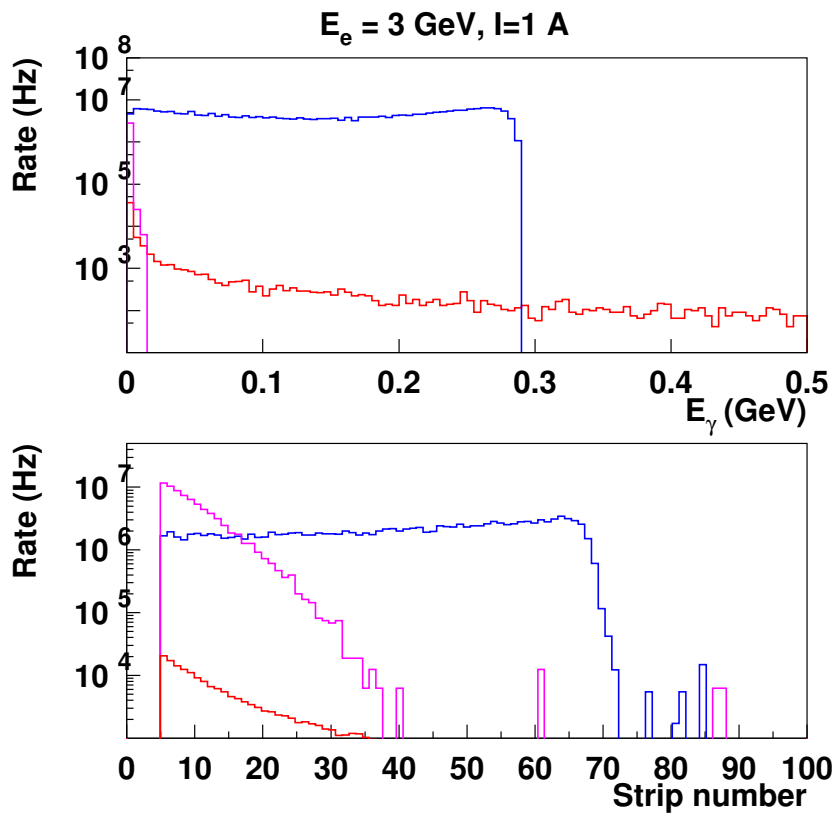


Figure 1: Compton signal and background for a 3 GeV beam and 1 kW green cavity. Blue = Compton Red = Bremsstrahlung Magenta=Halo

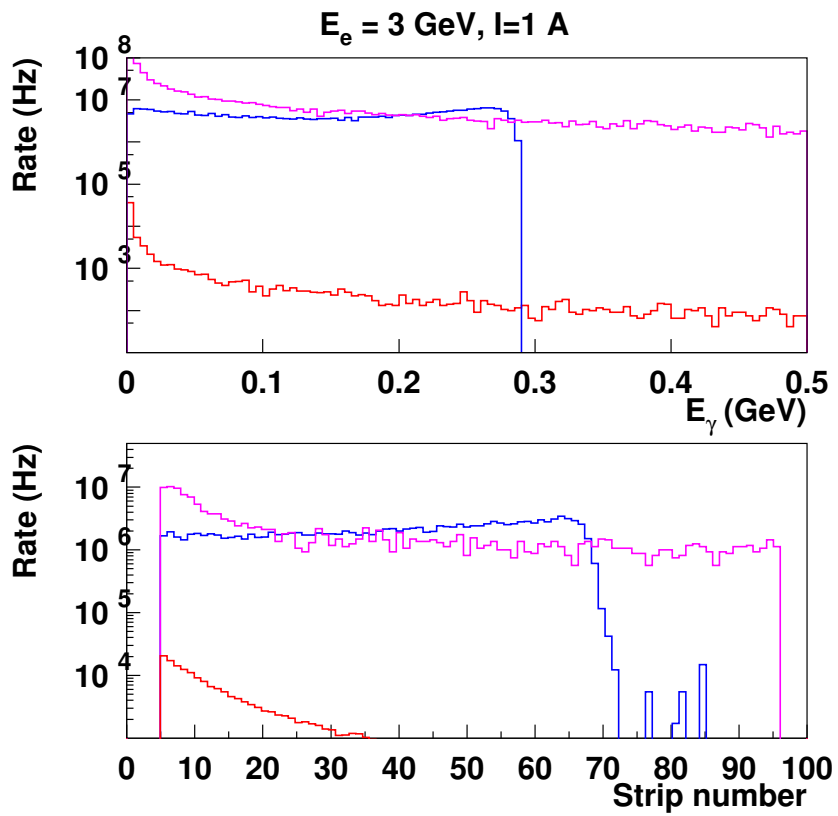


Figure 2: Compton signal and background for a 3 GeV beam and 1 kW green cavity. Blue = Compton Red = Bremsstrahlung Magenta=Halo

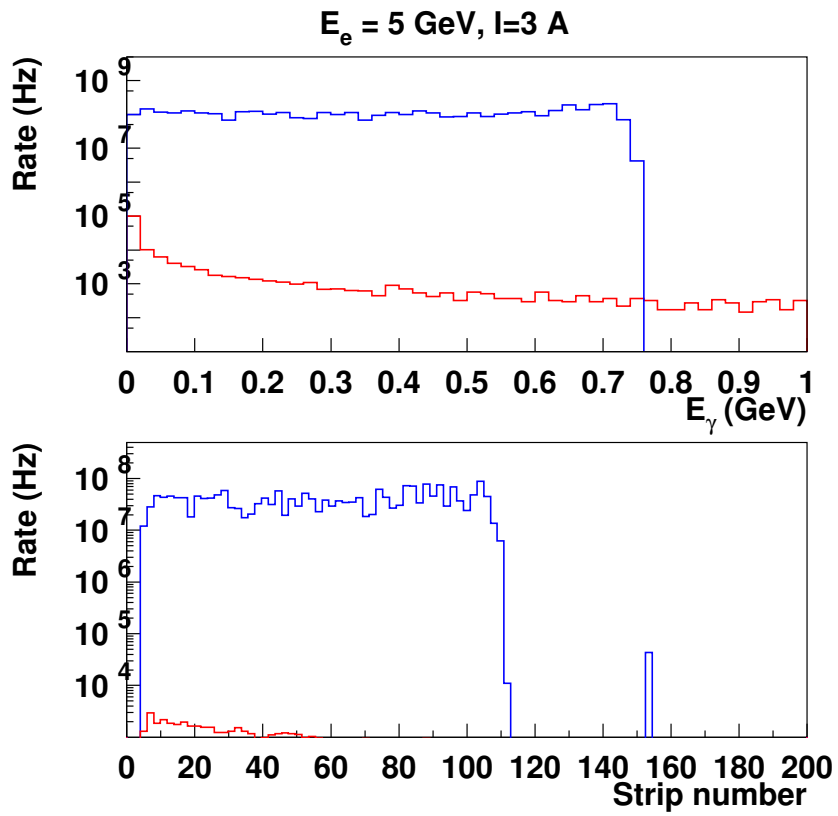


Figure 3: Compton signal and background for a 5 GeV beam and 10 kW green cavity with a 2 cm aperture. Blue = Compton Red = Bremsstrahlung Magenta=Halo

Machine	Energy	Rate (kHz/W/A)	Max current (A)	Rate kHz/W
MEIC	3	316	3	948
MEIC	5	298	3	894
MEIC	6	290	2	580
eRHIC	6	290	0.05	14.5
MEIC	7	283	1.1	311.3
eRHIC	7	283	0.05	14.15
MEIC	9	269	0.4	107.6
eRHIC	9	269	0.05	13.45
MEIC	11	258	0.18	46.44
eRHIC	11	258	0.05	12.9

From those number one can see that even with 1W only of laser power the Compton rates are significant and statistical accuracy can be reached in less than 1 second. Though we are keeping all laser options open since additional laser power might be required to overcome the background signals. In case of a 1 kW laser cavity rates will be of the order of several MHz. At this kind of rates an integrated measurement can be interesting to reduce the dead time and effect of pile up.

8 Electron Detector requirements

The EIC will have a much higher electron luminosity than any planned for Jefferson Lab at 12 GeV, with currents from 50 mA at eRHIC up to 3 A for MEIC. Radiation hardness for the detector active volume and electronics is absolutely essential. The maximum current at Jefferson Lab is on the order of 100 μA , with anticipated dose rates of 2 krad/hour per strip for the Hall A Compton electron detector, resulting from the signal electrons alone. For example, the MOLLER experiment will run at 11 GeV. Assuming a beam current of $I_e = 85 \mu A$ and a wavelength $\lambda = 532$ nm laser with a power $P_L = 1$ kW, the luminosity of the Compton interaction is

$$L = \frac{1 + \cos\alpha_c}{\sqrt{2\pi}} \left(\frac{I_e}{e}\right) \left(\frac{P_L\lambda}{hc}\right) \left(\frac{1}{c}\right) \left(\frac{1}{\sqrt{\sigma_e^2 + \sigma_\gamma^2}}\right) \left(\frac{1}{1 + \sin\alpha_c}\right) \quad (1)$$

where $\alpha_c = 1.4^\circ$ is the crossing angle and $\sigma_{e,\gamma}^2 = 80 \mu m$ are the size of the electron beam and the laser, respectively. The luminosity is $1.4 \times 10^{30} \text{ cm}^{-2}\text{s}^{-1}$ and the Compton scattered electron rate for MOLLER is about 70 kHz with these assumptions. Assuming $2 \text{ MeV cm}^{-2}\text{g}^{-1}$ energy deposition (approximately valid for both silicon and diamond) and a strip pitch of 0.24 mm over 4.6 cm (192 strips), the dose per strip is 1.8 Mrad over the life of the experiment (344 calendar days).

Adjusting for the size of the electron beam and laser in the Compton interaction region ($\sigma_{e,\gamma}^2 = 350 \mu m$), as well as the beam current (assume $I_e = 180$ mA,

the lowest MEIC current) the luminosity is $7.1 \times 10^{32} \text{ cm}^{-2}\text{s}^{-1}$, with a Compton scattered electron rate of 36 MHz. This results in a dose rate for a similar detector of 27 krad/hour (more than $10\times$ that for the MOLLER detector). For eRHIC this dose will be of the same order with 7.5 krad/hour. Assuming continuous running for 6 months in eRHIC case would give a minimum of 32.4 Mrad just from the Compton signal. Typical Si detectors have a signal to noise ratio divided by two after an exposure of 3 Mrad.

In addition to the Compton signal background rates from synchrotron radiation and Bremsstrahlung will also scale with current. For example during the QWeak experiment the Compton Photon detector had a signal to background ratio of 1 to 1. This will result in high counting rates and radiation damages from both signal and background.

9 The Jefferson Laboratory Compton polarimeters

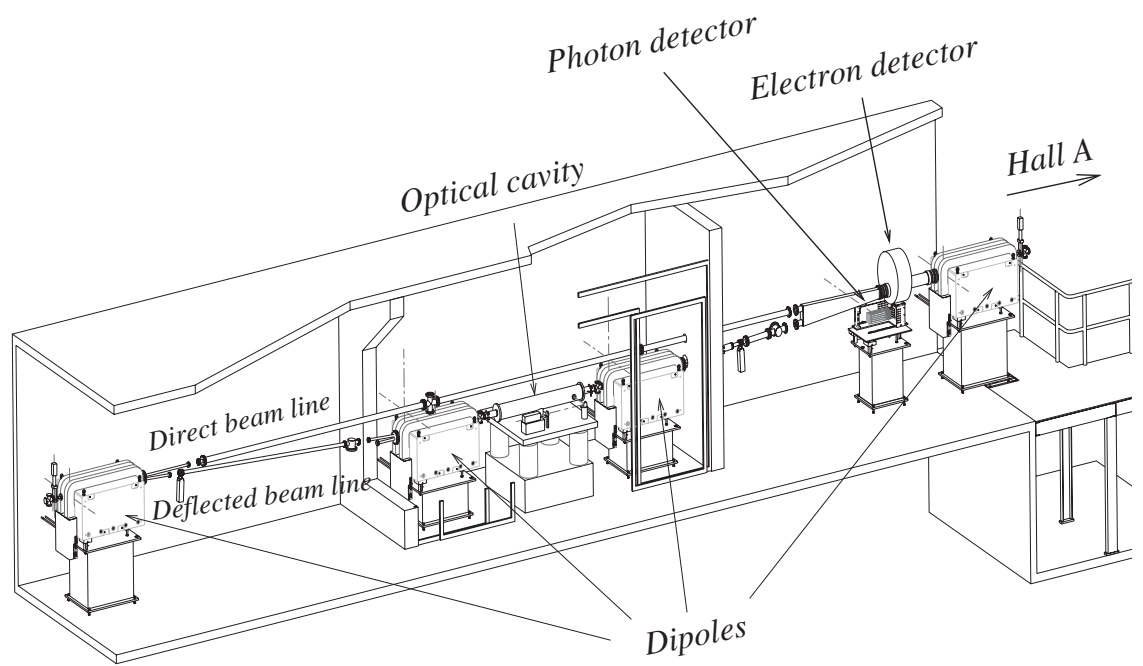
9.1 Parity violation program

The Jefferson Laboratory has a vast parity violating measurement program. Those measurement are sensitive to the parity violating nature of the Weak interaction. Usually those experiment have very high rates and measure asymmetries reaching of the order of part per million level. Such experiments are designed to not be statistically limited so all the systematics error are limiting the final accuracy of the measurement. Latest experiments required 1% accuracy which was achieved for HAPPEXIII, PREX. Several experiment are approved in particularly the Moller experiment which aims at 0.5 % accuracy on polarimetry. So EIC would benefit from the research and development of this program on polarization. Jefferson Laboratory would be a perfect testing ground since the energy range overlaps with both EIC machines.

9.2 Experimental setup

Both polarimeters at Jefferson Laboratory have a magnetic chicane. Four identical dipoles displace the beam to interact with the photon source : a Fabry-Perot cavity in the case of Hall A and C.

After a Compton interaction, the Compton photon is boosted forward and can be detected by a calorimeter. The Compton electron having lost energy will be deflected more by the third dipole of the chicane and will be displaced from the beam. By measuring this displacement one can measure the energy of the electron which corresponds to the Compton photon energy.

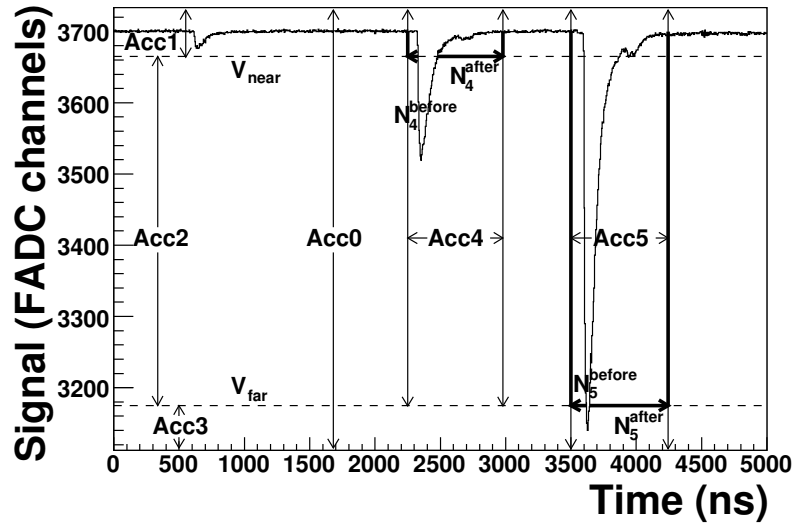


ht!

Figure 4: Hall A Compton chicane [18]

10 Photon detection polarimetry : Flash ADC based integrated method

The Hall A Compton photon calorimeter is based on a large GSO crystal read-out by a flash ADC. This crystal was optimized for low energy running of PREX experiment at 1 GeV . In order to eliminate the usual systematic due to calibration of the detector a digital integration method was tested.



For each helicity window all the samples are summed giving the integrated energy of the Compton spectrum. By doing the same for the other helicity as seen on fig, one can generate the integrated Compton asymmetry.

The polarization measurement for HAPPEX III [17, ?, 16] reach a 1% error measurement at 3 GeV. This is the best photon measurement achieved so far. This method is promising for EIC but the calorimeter will have to be upgraded for the higher energy to reduce leakage and the effect of background such as Brehmstrahlung can be more important at higher energies.

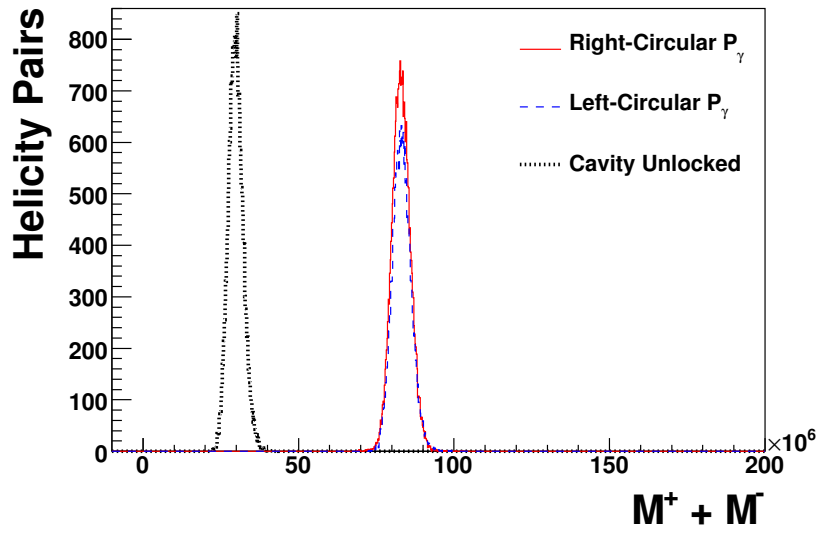
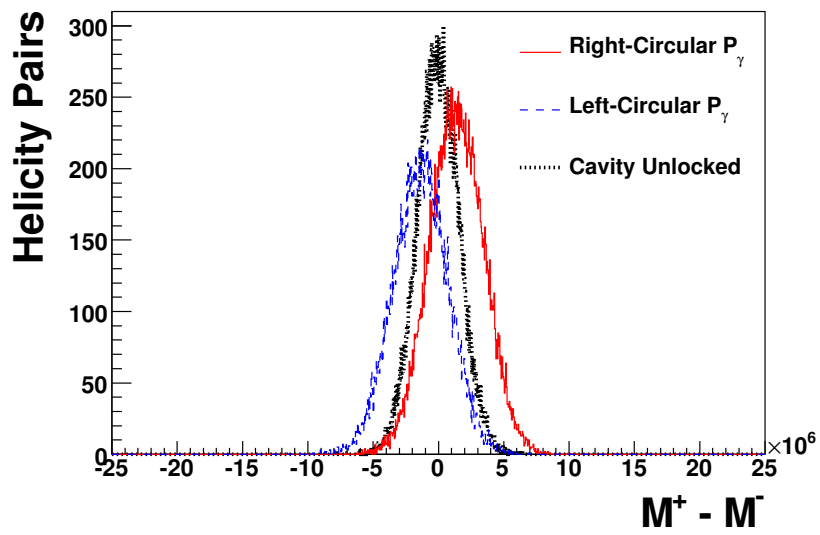
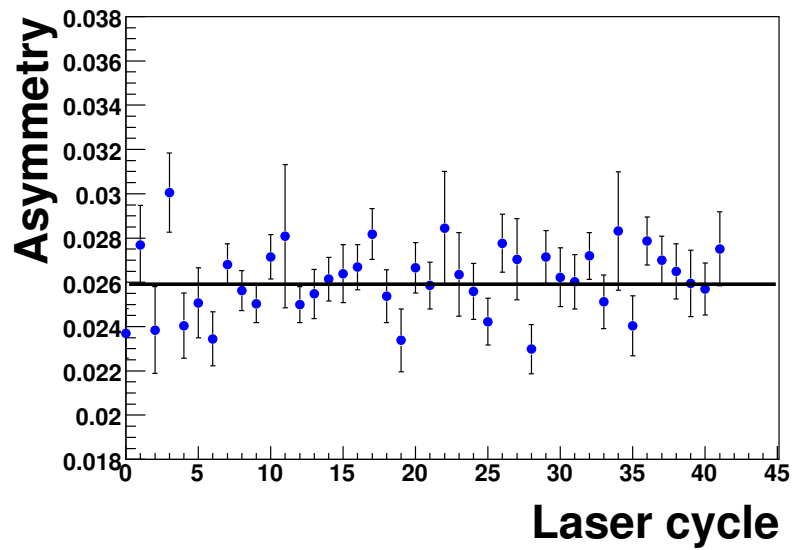
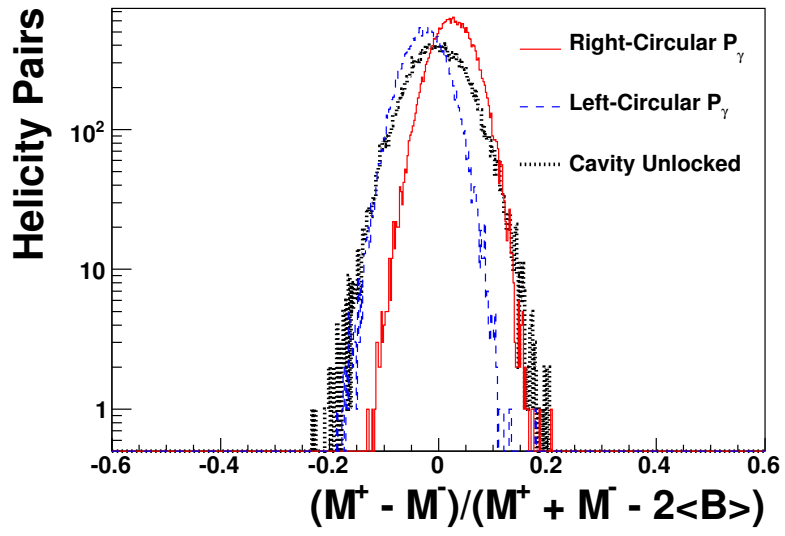
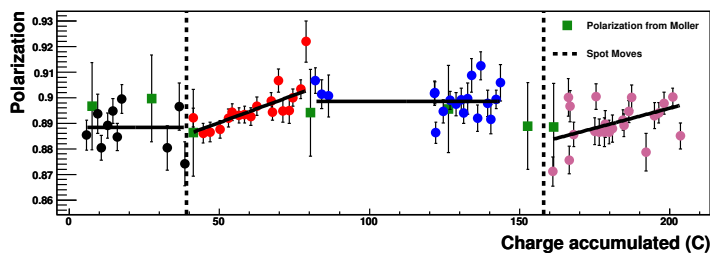


Figure 5: Sum of the integrals for different helicities







11 Electron detection polarimetry

The energy of the scattered Compton electron is known by measuring its deflection at the third dipole. By having the asymmetry as a function of energy one can fit the asymmetry and extract the polarization. The main systematic of this method is the energy calibration which give an uncertainty on the fit hence on the polarisation. This can translate in accuracy greatly depending on the geometry and knowledge of the magnetic field. A new method was used for the Hapex II experiment and HAPPEX He4, the Compton asymmetry has a zero crossing which can accurately be computed. By using this point and the Compton edge one has a self calibrating measurement. The remaining systematics error can be well controlled as seen in QWeak Hall C result using the electron detector in the section 11.2.

11.1 Experience from Hall A Silicon detector

The Hall A Compton detector was based on Silicon detector strips. An upgraded detector with a thinner pitch was installed. Several issues where found as far as background is concerned. The detector could not operate with a significant amount of shielding which can generate background in the detector. Also the dark current steadily increased with beam operation, the increase being slower as the amount of shielding is bigger. Though a contamination of the asymmetry due to the shielding was observed. The silicon detector have two main issues : sensitivity to background (low energy photon background) and radiation hardness. The results obtained from the Hall C electron detector are make us lean toward a more radiation hard detector such as diamond or quartz detectors.

11.2 Diamond as detector material

The use of diamond as detector material is a direct result of the development of the process known as chemical vapour deposition (CVD), which made it possible to obtain, thin sheets of centimeter size diamonds, at a reasonable cost. In the CVD process, a microwave-generated plasma or one of several other techniques is used to generate free radicals in the gas phase typically containing hydrocarbon gases and hydrogen and usually at low pressure. Under suitable conditions, these free radicals from the gas phase adhere to a pre-existing diamond surface (substrate) and a thin layer of the material is gradually built up by deposition [1]. Using the CVD process, it is possible to make plates of diamond resembling the ubiquitous silicon wafers used in the electronics industry. The diamond plates are then polished and cleaned to yield the blanks from which detectors can be made by the deposition of suitable electrodes on the surface [2]. A minimum ionizing particle (MIP) passing through a thin layer of diamond loses just a small fraction of its initial kinetic energy, but leaves behind a trail of electronhole pairs. In the presence of an external electric field, the electrons and holes move away from one another, and this movement of the charges induces a signal in the external circuit. A MIP produces about 36 electron-hole pairs per μm it travels through the diamond. The signal per electronhole pair is proportional to the mean separation of the electron and hole before they become trapped in the material, also known as the charge collection distance. The charge collection distance in detector grade poly-crystalline diamond is $\sim 250\mu\text{m}$ for electric fields of $1\text{V}/\mu\text{m}$ and higher. This implies that the signal size in a diamond detector is significantly smaller than the signal size in a silicon detector. However, because of the higher electron and hole mobility of diamond compared to silicon the signal is faster and of smaller duration. The well-established resistance of diamond to damage by radiation is by far the most important reason for considering the use of diamond detectors in nuclear and particle physics experiments. The effect of radiation damage on doped silicon is effectively to remove donor sites which leads to increase of the leakage current and can ultimately produce “type inversion.” [3] As diamond is not doped, it does not suffer from these type of radiation damage. The radiation hardness of diamond has been studied systematically via exposure to gamma rays, electrons, pions, protons, alpha particles and neutrons [4, 5]. In all cases the charge-collection distance was measured at various stages during the exposure. In one such study, a diamond detector exposed to a 2.2 MeV electron beam with a total dose of 100 MRad [5], showed no evidence of signal degradation. In a different study a diamond detector irradiated with protons to a dose of 50 Mrad resulted in a 15% reduction in signal-to-noise [6].

11.3 The Jefferson Lab, Hall-C diamond microstrip detector

Recently, a new Compton polarimeter was installed in Jefferson Lab, Hall-C to continuously monitor the electron beam polarization. The polarimeter was

used during the QWeak experiment which aims to measure the weak charge of the proton with an uncertainty of 4% [7]. The polarimeter uses Compton scattering between circularly polarized photons from a 532 nm laser and the polarized electron beam, with both the scattered photons and the recoiling electrons being detected. The recoil electrons from the Compton scattering process were momentum analyzed in a dipole magnet and detected by a set of four diamond micro-strip detectors. These detectors are made from 21 mm \times 21 mm \times 0.5 mm plates of CVD diamond [8]. Each diamond plate has 96 horizontal electrode strips with a pitch of 200 μ m (180 μ m of metal and 20 μ m of gap) on one side (front) and a single metalized electrode covering the entire diamond surface on the opposite (back) side. The electrodes consist of successive depositions of Ti, Pt and Au [9]. Each diamond plate was mounted on a 60 mm \times 80 mm Alumina substrate using a silver epoxy that made a robust electrical contact between the back side of the detector plate and a miniature HV connector on the Alumina substrate. Each of the 96 strips on the front side of the diamond detector was wire bonded to Gold traces on the alumina substrate with twin strands of 5 μ m Al wires. The gold traces terminated on two 50-pin high density connectors placed on either side of the detector plate. The 48 even strips were all connected to one high density connector while the 48 odd strips were connected to the second. One pin on each high density connector was electrically connected to a grounding layer on the Alumina substrate. A single detector plane is shown in Fig 6 (left panel).

The four detector plates were mounted inside a vacuum can, with a spacing of \sim 1 cm between each plate and an inclination of \sim 10.2 $^\circ$ with the vertical, such that the detectors were approximately perpendicular to the path of the electron beam through the dipole magnet. The stack of detectors was attached to a vertical linear feedthrough with a 12-inch travel. Under operating conditions the detectors were lowered to a vertical distance of \sim 7 mm from the main electron beam. When not in use the detectors were retracted away from the beam, into a section of the vacuum chamber (garage) that was shielded with a lead plate. and a bias voltage of \sim 400 V is maintained across each detector plane. The detector signal (typically \sim 9000 e $^-$) is carried outside the vacuum can via a set of 55 cm long, 5-layer, flexible printed circuit boards made out of Kapton, that connect the detectors to a set of 50-pin vacuum feedthroughs. The air-side of these feedthroughs were used as the backplane for two, forced-air cooled, euro-card crates that held a set of custom pre-amplifier and discriminator cards built by the tri university meson facility (TRIUMF). Each of these cards known as Qweak amplifier discriminator cards (QWADs) consist of a chain of 48 low-noise pre-amplifiers, shaping amplifiers and discriminators. The polarity of each QWAD channel is individually selectable and the discriminator threshold is adjustable over a range of \pm 40 mV. The pre-amplifiers have a typical gain of 100mV/fC, the shaping amplifier has a width of \sim 0.6 μ sec and the discriminators produce a LVDS output.

The signal pulses from the detector planes were amplified, shaped and digitized by the QWAD modules. The digital signals from the QWADs are carried to the data acquisition system via 200 ft of cable, where the detector signals were

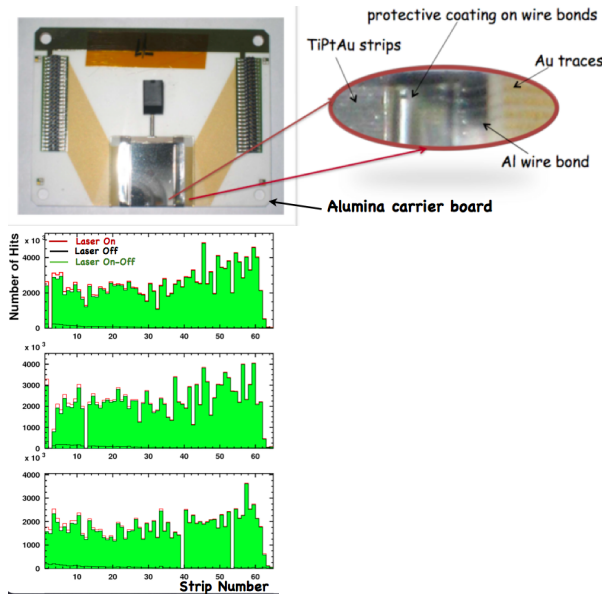


Figure 6: (left) The CVD diamond plate mounted on an alumina substrate which forms a single detector plane. (right) A spectrum of hits on each strip of the 3 active detector planes.

grouped into 3 clusters of 32 strips each. The digital signals are processed using a set of four field programmable gate array (FPGA) based general purpose logic boards. The upper, middle and bottom clusters from the 4 detector planes are each processed on a single slave logic board. In each of the 3 slave logic boards the signals are reconditioned, and split into two copies. One copy is used to form a trigger for each detector plane based on a pseudo-tracking algorithm, while the other copy is delayed. The trigger from each detector plane is processed by the master logic board to form the final trigger decision (one, two or three plane trigger) which is then used to permanently record the appropriate delayed copy of the signal. The entire data acquisition is controlled using the ceba online data acquisition (CODA) system [?].

The data were collected in ~ 1 hr long runs which were later decoded and used to fill histograms of hits on each detector strip. Only 3 out of the 4 detector planes were operational during the experiment. The typical strip hit spectra are shown in Fig 6 (right panel). These histograms were filled for the two electron helicities and the laser off data are used to build the background spectra. Using the background corrected strip hit spectra for each electron helicity state was used to obtain the asymmetry as a function of the deflected electron momentum. The asymmetry spectra were compared with an exact calculation to obtain the electron beam polarization. A typical asymmetry spectra along with the QED calculation is shown in Fig 7. The beam polarization obtained

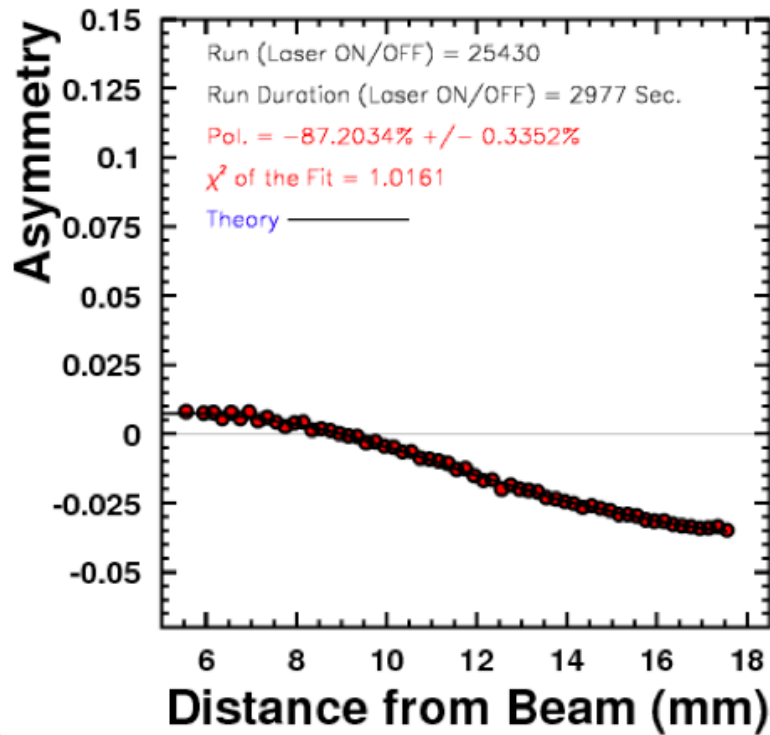


Figure 7: A spectrum of the measured asymmetry along the the QED calculation shown by the solid line.

using the electron detector were found to be consistent with the measurements performed at lower currents using a Moller polarimeter. The desired statistical precision of $< 1\%$ per hour was achieved and it is expected to achieve the $\sim 1\%$ systematic precision. By comparing the expected to the observed rates the detector efficiency was estimated to be $\sim 70\%$. The large inefficiency is mostly due to the large separation between the detector and the readout electronics. Over the 2 year period of the QWeak experiment, the detectors were exposed to a radiation dose of ~ 10 Mrad. No significant degradation of the signal size was observed during this period.

12 Quartz integrating detector

Fused silica (so called “quartz”) Čerenkov detectors with PMTs have been used for decades in various high rate applications. These applications include hadronic particle ID systems and calorimeters, luminosity monitors, and high rate electron flux integrators for precision electroweak and parity violating electron scattering experiments. The fused silica used in these detectors are high purity SiO₂ and prized for their ability to maintain excellent near-UV transmission under severe (Grad) radiation exposure [10]. The fused silica brand of choice is Spectrosil 2000 which is manufactured using a proprietary process of melting high purity silica sand.

The specific type of quartz detector we are considering for the electron detector is a “thin” quartz detector. That is, the amount of quartz traversed by scattered electrons is only ~ 1 cm. This makes for a more consistent light pulse per electron yielding better overall integrated resolution; the drawback is the light pulse is not as bright for thin quartz detectors. However, the nature of the Čerenkov detection mechanism makes these detectors relatively insensitive to gamma ray and other neutral backgrounds.

The initial design of the quartz electron detector will be based on the PREX detector design. It will use a single piece of quartz coupled to a 2 inch PMT using an aluminum mirror air light guide. Figure 8 shows a schematic of two prototype designs. For both designs, the quartz bar is 14.0 cm \times 3.5 cm \times 1.0 cm with a 45° bevel on one end. The bar is Spectrosil 2000 with a standard optical polish on all six sides. The prototype design shown in Figure 8 (left) has been the subject of extensive Monte Carlo studies and cosmic ray bench tests and can produce 60-70 photo-electrons per incident particle. For this design, particles pass through the quartz at a 45° angle with respect to the plane of the quartz. This allows roughly half the Čerenkov light cone to go directly to the PMT, while the other half is mostly lost. Figure 8 (right) shows a new design concept for the thin quartz detector. This design, in theory, can direct the entire Čerenkov cone to the PMT using the nearly perfect total internal reflection inside the quartz. A version of this design was recently tested at Mainz using MAMI’s 800MeV electron beam with very promising results.

Since the rates reach the MHz level of signal we can think of using such a detector for Compton measurement. The PMT would be readout using a FADC using the same technique as use for the photon calorimeter allowing to take event by event data or integrated data at high rate. Having an integrated method has the main advantage is that there is no dead time correction and the detector can handle multievent pile up. The main drawback is the sensitivity to the background and to electronic noise, this method will work well if the signal over background is well-known.

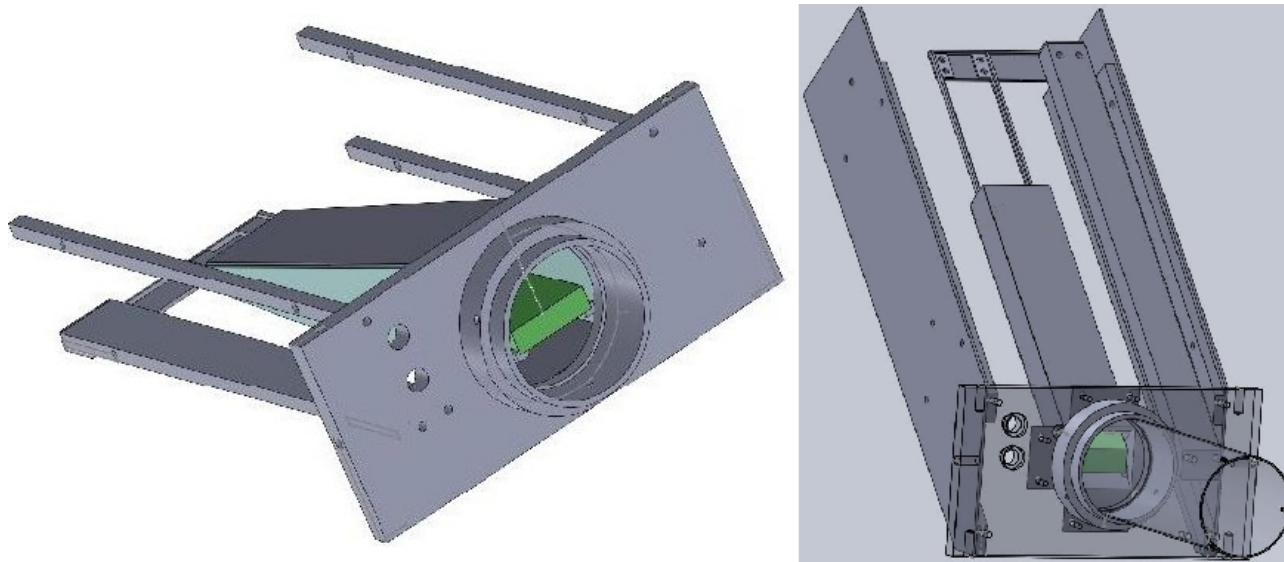
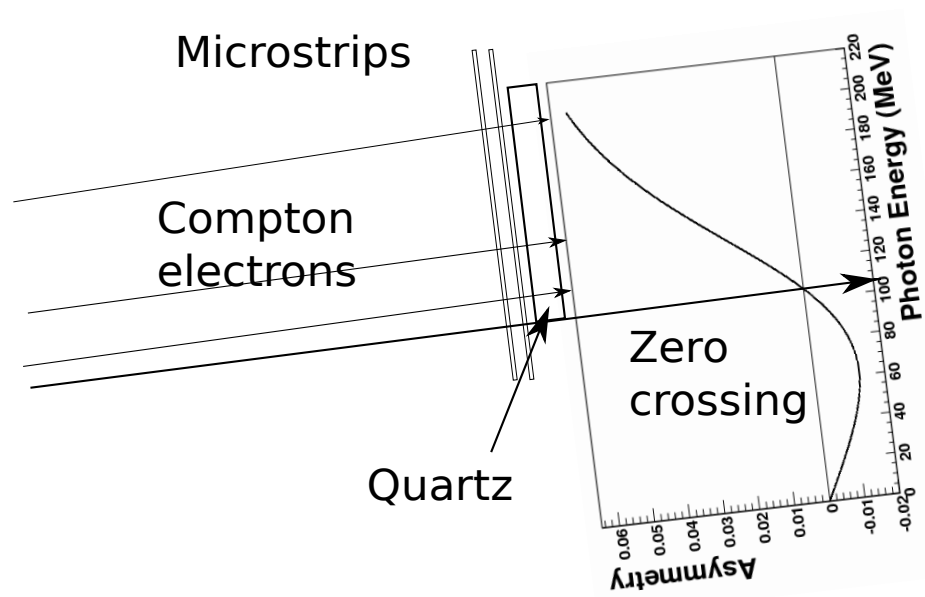


Figure 8: Prototype thin quartz detector designs: (left) Design is similar to PREX detector where the quartz and PMT lie in the same plane. (right) Design is new improved design which gives more light and better resolution. Quartz bars are shown in green.



The detector will be paired with a tracking detector placed in front to determine its position accurately with respect to the zero crossing of the asymmetry. We will place the edge of the quartz close to the zero crossing to minimize the change in asymmetry due to the position accuracy. The systematic error will come from the position of the edge of the quartz with respect to the Compton asymmetry zero crossing. For example at 11 GeV and assuming a strip width of $250 \mu\text{m}$ we have a 0.3 % error on the total asymmetry. This error could be reduced with better position resolution. After the alignment is done at lower current, the detector could be used at full current. The positioning detector could be run at the same time at lower HV to reduce the efficiency or also in integrating mode.

In a first step, the detector will be tested in vacuum with a silicon based readout. This will be procured in the first year. First tests will reuse already existing pieces of quartz. Additional simulation and design will be done to look at optimization of light collection, optimization of the geometry and the possibility of segmenting the detector.

The Micromesh Gaseous Detectors (Micromegas) are a particular type of micropatterned gaseous detectors. They are constituted of a cathode plane and a drift space filled with a gas. Charged particles will generate ionization and the electrons created will drift toward the readout following the electric field. The readout is a usual plastic circuit board with metallic strips. A metallic micromesh is placed at a few hundreds of microns from the readout board and it is put at high voltage creating a very high field between the mesh and readout. The electrons are accelerated in this field and will multiply in the gas amplifying the signal to be readout. A new industrial process called “bulk” Micromegas has been used to produce the detectors, it consists of laminating the mesh on the readout circuit board covered by a photoresist layer. A mask is then applied and the detector is insulated with UV. After development the photoresist left forms small pillars holding the mesh. This result in a simple and sturdy detector. There are several advantages of the process :

- the raw materials are cheap and available in industrial quantities.
- the production is quick, a detector can be produced in one day which reduces the cost in labor for mounting
- the detector can be produced rapidly in mass and on demand which is an advantage over the long lead time which can occur for the GEM foils procurement.

One main drawback with the Micromegas compared to the GEM because the amplification space is extended all along the mesh detector is the sparking. This issue is improved by adding a resistive layer on the readout strips and is being evaluated.

Two prototypes are proposed. One is an adaptation of the silicon microstrip design using Micromegas.

The PCB will be build with same pitch as the silicon detector and with the same number of channels. A second PCB will constitute the frame and a foil of mylar will close the detector creating a small volume for the gas. The detector will be compatible with the current silicon electronics to allow quick testing. The Micromesh Gaseous Detector (Micromegas) are a cheaper alternative to silicon or diamond. The second design is a modular micro drift chamber allowing very high radiation hardness and easy servicing of the detector. It consists of a volume of gas with a cathode plane on the right side and the readout plane on the left side based on Micromegas. The Compton electrons will produce ionization which will drift toward the readout where they will be multiplied and detected on the Micromegas readout.

This detector will be ideal in a roman pot where the volume could be filled with gas. The high rates of particles will not go through the readout prevent

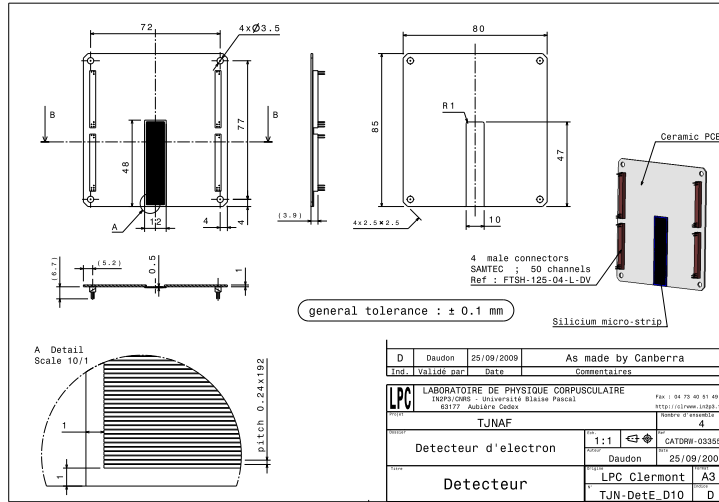
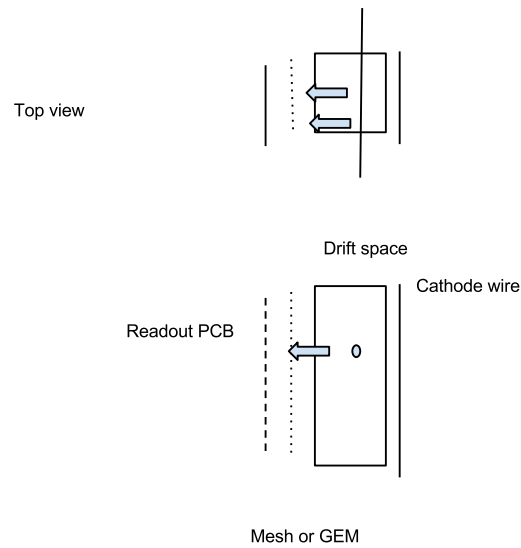


Figure 9: Hall A Compton electron silicon detector drawing



radiation damages. The main potential aging could come from the mesh and readout but this part will be designed to be easily replaced.

12.1 Roman pot

The roman pot technique was introduced at CERN. It consists of a secondary chamber moving inside the vacuum where the detector are placed. A system of compensation will be used to balanced the large force from the vacuum on the surface of the chamber. This technique is routinely used at CERN for very small angle measurements with detectors as close as 1 mm from the beam. A thin window is machined in the bulk of the secondary vacuum chamber to reduce the material in the path of the particles of interest. In the case of the Compton interaction, the Compton events are along a stripe in the dispersive plane of the dipole with a width of about 5 mm by 5 cm long depending on where the dispersion of the magnet and where the detector is located.

12.2 Implementation for the Compton electron detector

The Roman pot technique has several advantages :

- the detector could be operated at atmospheric pressure allowing to use gaseous detectors
- the detectors moves with the pot which can reduce the cable length between detector and electronics since no vacuum feedthrough are needed. This potentially could improve the diamond detector efficiency.
- detector can be accessed easily for servicing and swapping

The major drawback is the contribution of the thin window interacting with the electrons which could change the shape of the Compton asymmetry because of rescattering of electrons inside it.

The chamber could be designed to hold detectors both in the pot and in the vacuum to compare the effect of the vacuum window of the pot.

Following is a conceptual drawing of a possible roman pot.

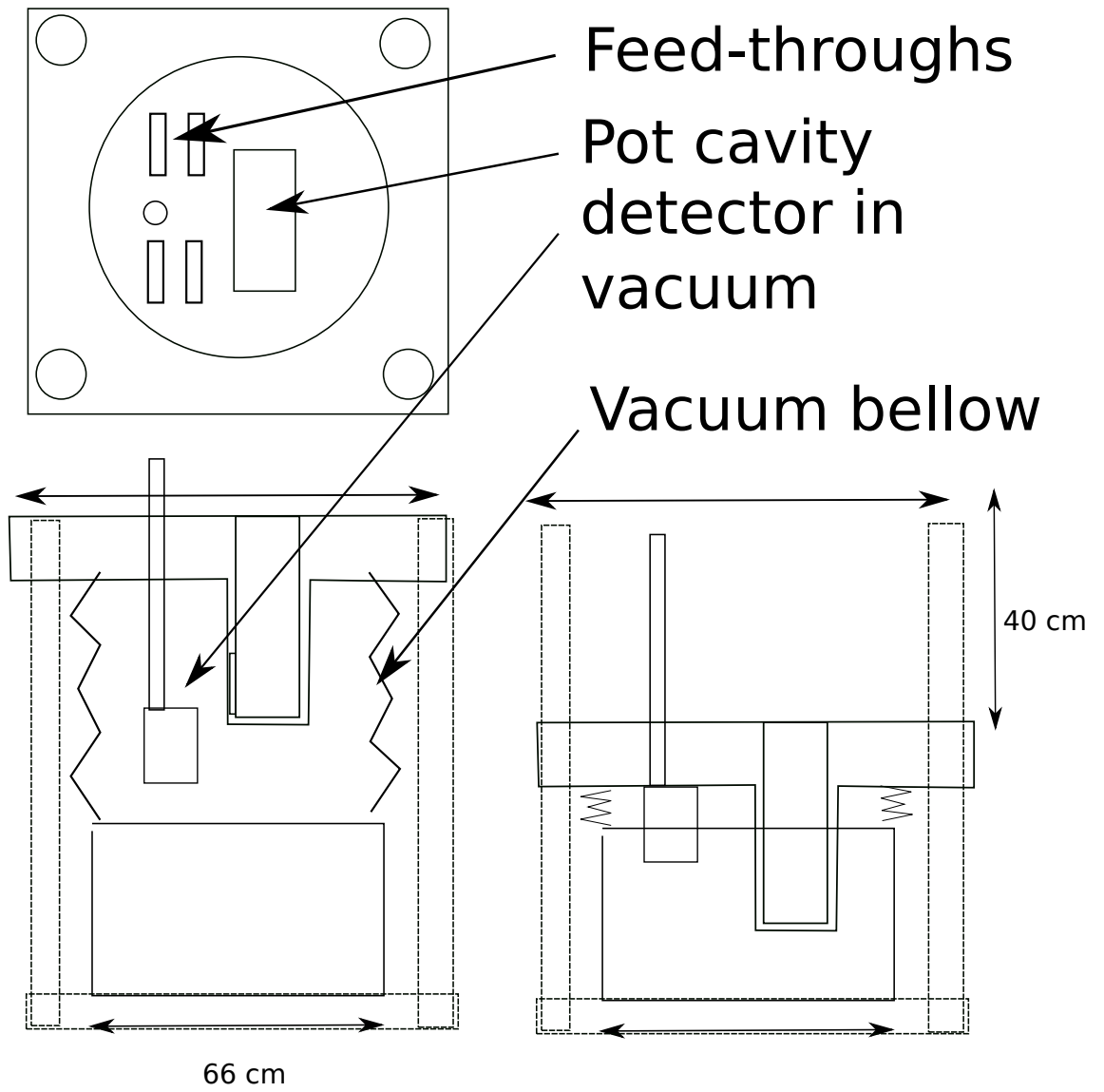


Figure 10: Test detector Roman pot conceptual design

13 Additional resources

A proposal will be put at Jefferson Laboratory LDRD program for total or partial funding for the roman pot. Many of the R&D project will reuse resources and manpower from parity collaboration. For examples FADC hardware and software developed by CMU and William and Mary. Amplifier Discriminator electronics used by QWeak experiment. Quartz detector from Idaho State University... Budget will be reduced depending on the additional funding the collaborators. Resources for the Roman pot chamber could also be shared with the Roman pot R&D design.

References

- [1] M. Werner and R. Locher Rep. Prog. Phys. **61**, 1665 (1998).
- [2] R. J. Tapper, Rep. Prog. Phys. **63**, 1273 (2000).
- [3] J. A. J. Matthews *et al.* Nucl. Instrum. Methods **A381**, 338 (1996).
- [4] C. Bauer *et al.* Nucl. Instrum. Methods **367**, 207 (1995).
- [5] M. M. Zoeller *et al.* IEEE Trans. Nucl. Sci. **44** 815 (1997).
- [6] F. Hartjes, 3rd Int. Conf. on Radiation Effects on Semiconductor Materials, Detectors and Devices (Florence, 2000)
- [7] R. Carlini *et al.*, arXiv:1202.1255
- [8] The CERN grade diamond plates were procured from Element Six, 35 West 45th St., New York, NY 10036, USA.
- [9] The diamond plates were metalized and wire bonded by Diamond Detectors Limited, 16 Fleetsbridge Business Centre, Upton Road, Poole, Dorset, BH17 7AF, UK.
- [10] B. Grosdidier, CRN 92-45 (1992); D. Lazic, CRN 93-48 (1993)
- [11] D. Wang *et al.* [PVDIS Collaboration], Nature **506**, no. 7486, 67 (2014).
- [12] S. Abrahamyan, Z. Ahmed, H. Albataineh, K. Aniol, D. S. Armstrong, W. Armstrong, T. Averett and B. Babineau *et al.*, Phys. Rev. Lett. **108**, 112502 (2012) [arXiv:1201.2568 [nucl-ex]].
- [13] M. Friend [HAPPEX Collaboration], Nuovo Cim. C **035N04**, 137 (2012).
- [14] M. Friend, G. B. Franklin and B. Quinn, Nucl. Instrum. Meth. A **676**, 66 (2012) [arXiv:1108.3096 [physics.ins-det]].
- [15] C. J. Horowitz, Z. Ahmed, C. M. Jen, A. Rakhman, P. A. Souder, M. M. Dalton, N. Liyanage and K. D. Paschke *et al.*, Phys. Rev. C **85**, 032501 (2012) [arXiv:1202.1468 [nucl-ex]].
- [16] M. Friend, D. Parno, F. Benmokhtar, A. Camsonne, M. Dalton, G. B. Franklin, V. Mamyran and R. Michaels *et al.*, Nucl. Instrum. Meth. A **676**, 96 (2012) [arXiv:1108.3116 [physics.ins-det]].
- [17] Z. Ahmed *et al.* [HAPPEX Collaboration], Phys. Rev. Lett. **108**, 102001 (2012) [arXiv:1107.0913 [nucl-ex]].
- [18] J. Alcorn, B. D. Anderson, K. A. Aniol, J. R. M. Annand, L. Auerbach, J. Arrington, T. Averett and F. T. Baker *et al.*, Nucl. Instrum. Meth. A **522**, 294 (2004).